Self-Assembled via Axial Coordination Magnesium Porphyrin−Imidazole Appended Fullerene Dyad: Spectroscopic, Electrochemical, Computational, and Photochemical Studies

ARTICLE *in* THE JOURNAL OF PHYSICAL CHEMISTRY B · JUNE 2005

Impact Factor: 3.3 · DOI: 10.1021/jp050591l · Source: PubMed

Self-Assembled via Axial Coordination Magnesium Porphyrin−Imidazole Appended Fullerene Dyad: Spectroscopic, Electrochemical, Computational, and Photochemical Studies

Francis D'Souza,*,† Mohamed E. El-Khouly,‡,§ Suresh Gadde,† Amy L. McCarty,† Paul A. Karr,|| Melvin E. Zandler,† Yasuyaki Araki,‡ and Osamu Ito*,‡

Department of Chemistry, Wichita State University, 1845 Fairmount, Wichita, Kansas 67260-0051, Institute of Multidisciplinary Research for Advanced Materials, Tohoku University, Katahira, Sendai, 980-8577, Japan, Department of Chemistry, Graduate School of Science, Tohoku University, Aoba, Sendai 980-8587, Japan, and Department of Chemistry, Wayne State College, 1111 Main, Wayne, Nebraska 68787

Received: February 2, 2005; In Final Form: March 24, 2005

Spectroscopic, redox, and electron transfer reactions of a self-assembled donor−acceptor dyad formed by axial coordination of magnesium *meso*-tetraphenylporphyrin (MgTPP) and fulleropyrrolidine appended with an imidazole coordinating ligand (C_{60}Im) were investigated. Spectroscopic studies revealed the formation of a 1:1 C_{60}Im:MgTPP supramolecular complex, and the anticipated 1:2 complex could not be observed because of the needed large amounts of the axial coordinating ligand. The formation constant, K_1, for the 1:1 complex was found to be $(1.5 \pm 0.3) \times 10^4$ M^{-1}, suggesting fairly stable complex formation. The geometric and electronic structures of the dyads were probed by ab initio B3LYP/3-21G(*) methods. The majority of the highest occupied frontier molecular orbital (HOMO) was found to be located on the MgTPP entity, while the lowest unoccupied molecular orbital (LUMO) was on the fullerene entity, suggesting that the charge-separated state of the supramolecular complex is $C_{60}Im^{\bullet-}$:$MgTPP^{\bullet+}$. Redox titrations involving MgTPP and C_{60}Im allowed accurate determination of the oxidation and reduction potentials of the donor and acceptor entities in the supramolecular complex. These studies revealed more difficult oxidation, by about 100 mV, for MgTPP in the pentacoordinated C_{60}Im:MgTPP compared to pristine MgTPP in *o*-dichlorobenzene. A total of six one-electron redox processes corresponding to the oxidation and reduction of the zinc porphyrin ring and the reduction of fullerene entities was observed within the accessible potential window of the solvent. The excited state events were monitored by both steady state and time-resolved emission as well as transient absorption techniques. In *o*-dichlorobenzene, upon coordination of C_{60}Im to MgTPP, the main quenching pathway involved electron transfer from the singlet excited MgTPP to the C_{60}Im moiety. The rate of forward electron transfer, k_{CS}, calculated from the picosecond time-resolved emission studies was found to be 1.1×10^{10} s^{-1} with a quantum yield, Φ_{CS}, of 0.99, indicating fast and efficient charge separation. The rate of charge recombination, k_{CR}, evaluated from nanosecond transient absorption studies, was found to be 8.3×10^7 s^{-1}. A comparison between k_{CS} and k_{CR} suggested an excellent opportunity to utilize the charge-separated state for further electron-mediating processes.

Introduction

The X-ray structures of the bacterial photosynthetic reaction centers have revealed that the electron donor and acceptor entities are arranged via noncovalent incorporation into a well-defined protein matrix.[1] The light induced electron transfer and energy transfer events occur between these well-organized pigments with a high quantum efficiency.[1] Development of relatively simple donor−acceptor model systems designed to mimic the events of the photosynthetic reaction center has been one of the important goals of chemistry during the past two decades.[2−8] To increase the rate of forward electron transfer and to slow the charge recombination (charge separation), improved model compounds with well-adjusted energies of the donor and acceptor molecules and finely tuned electronic coupling between the donor and acceptor entities have been elegantly designed and studied. In some cases, long-lived charge-separated states have been achieved by incorporating secondary electron donor or acceptor entities into multicomponent arrays such as triads, tetrads, and pentads.

Fullerenes have been widely utilized as electron acceptors.[8] Among the different properties, the reduction potentials and the small reorganization energy associated in electron transfer reactions of fullerenes are important properties for building donor−acceptor systems. While the first reduction potential of fullerene (C_{60}) is comparable to the widely used benzoquinone acceptor, the small reorganization energy is due to fullerene's unique structure and symmetry, which is ultimately responsible for its high degree of electron delocalization and structural rigidity. Generally, the forward electron transfer occurs in the "normal region" of the Marcus parabola, while the charge recombination occurs in the "inverted region" of the Marcus curve for electron transfer involving porphyrin−fullerene dyads.

Zinc porphyrins and zinc phthalocyanines have been widely utilized to construct donor−fullerene dyads.[8,9] Several covalently

* To whom correspondence should be addressed. E-mail: Francis.DSouza@wichita.edu (F.D'S.); ito@tagen.tohoku.ac.jp (O.I.).
† Wichita State University.
‡ Institute of Multidisciplinary Research for Advanced Materials, Tohoku University.
§ Graduate School of Science, Tohoku University.
|| Wayne State College.

10.1021/jp050591l CCC: $30.25
Published on Web 04/21/2005

CHART 1: Structures of the 1:1 and 1:2 Supramolecular Complexes of MgTPP and C_{60}Im

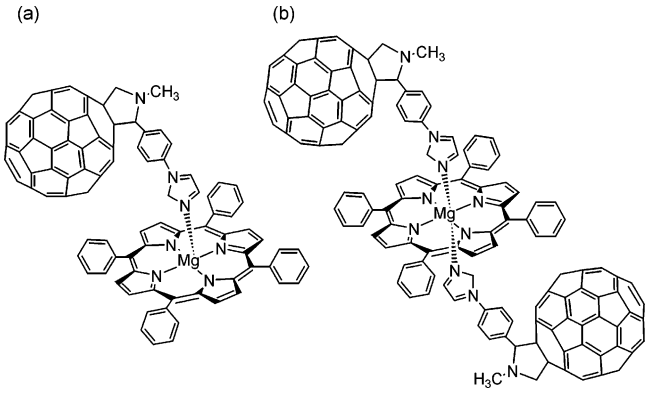

and noncovalently linked zinc macrocycle−fullerene dyads have been synthesized and studied. Among the different noncovalent binding approaches, zinc-to-ligand axial coordination by a fullerene functionalized to possess a nitrogenous ligand is one of the most popular approaches.[9] "Simple" supramolecular dyads involving just one mode of binding to "complex" supramolecular dyads and triads involving more than one mode of binding have been developed and studied by this approach. The complex supramolecular dyads and triads were designed to control the distance and orientation of the entities and also to create long-lived charge-separated states.[9−13]

To further our understanding of the structure−reactivity aspects and the associated free-energy changes on photoinduced charge separation and charge recombination, varying the metal ion of the porphyrin cavity is another choice of interest. However, only a handful of metalloporphyrins are fluorescent.[14] Among them, magnesium porphyrin is known to be a fluorescent compound possessing a diamagnetic metal ion in the porphyrin cavity.[15] Magnesium porphyrins offer a few advantages over the widely studied zinc porphyrins, viz., (i) higher fluorescence quantum yields and longer excited state lifetimes (5−10 ns of magnesium porphyrins versus 2−2.5 ns of zinc porphyrins),[20] (ii) easier oxidization of magnesium *meso*-tetraphenylporphyrin (MgTPP) due to the less electronegative magnesium (200 mV easier than ZnTPP), and (iii) the ability of MgTPP to bind up to two axial ligands, unlike zinc porphyrins which are known to bind one axial ligand.[16] Hence, the utilization of magnesium porphyrins in building self-assembled supramolecular donor−acceptor complexes is a topic of interest which has been explored here.

In the present study, we have utilized the well-established metal−ligand axial coordination approach to form a self-assembled magnesium porphyrin−fullerene(s) dyad (Chart 1). For this, a fullerene bearing an imidazole entity (C_{60}Im) has been employed to axially coordinate to magnesium tetraphenylporphyrin (MgTPP) in a noncoordinating solvent, *o*-dichlorobenzene. The imidazole appended fullerene has been chosen over the pyridine appended fullerene because of its increased ability to form stable coordination bonds with metal ions in the porphyrin cavity.[10,11] The binding constant, stoichiometry, and electronic structure were deduced from spectroscopic, computational, and electrochemical studies. Photochemical events occurring from the singlet excited MgTPP to axial coordinated fullerene in the supramolecular complex were monitored by steady state and time-resolved emission and nanosecond transient absorption studies.

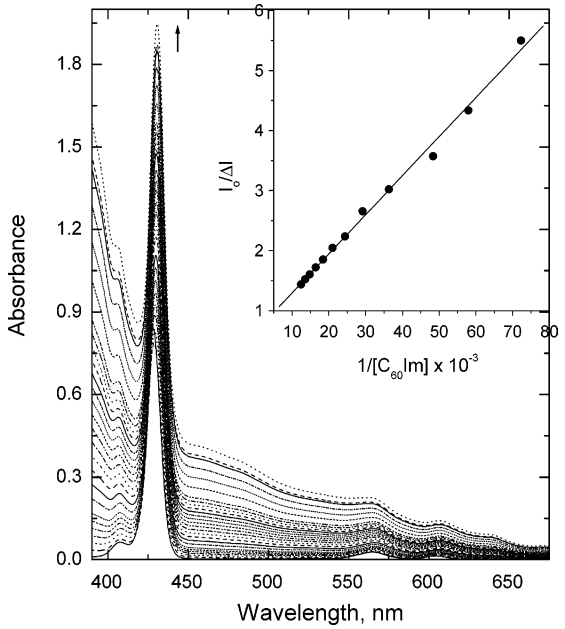

Figure 1. Spectral changes observed during the titration of MgTPP (6.62 μM) upon increasing addition of C_{60}Im (1.31 μM each addition) in *o*-dichlorobenzene. The inset shows the Benesi−Hildebrand plot for the change of absorbance at 430 nm.

Results and Discussion

Formation and Characterization of a Self-Assembled via Axial Coordination C_{60}Im−MgTPP Dyad. *Optical Absorbance Studies.* The spectral features of MgTPP are similar to those of ZnTPP in *o*-dichlorobenzene with an intense Soret band at ~430 nm and two visible bands located at 565 and 605 nm, respectively. It is known from the earlier studies that MgTPP upon pentacoordination exhibits an increased Soret intensity with slightly red shifted (3−6 nm) visible bands while the hexacoordinated MgTPP exhibits both red shifted Soret (shift of about 10 nm) and visible bands (10−18 nm shift).[16] Figure 1 shows the UV−visible optical absorption spectral changes observed during the complexation of C_{60}Im with MgTPP. Upon addition of C_{60}Im to a solution of MgTPP, the Soret band revealed an increased intensity while the visible bands were red shifted by <3 nm. The increase in the Soret band intensity was much more than that obtained by digital addition of the individual spectrum of MgP and C_{60}Im. These spectral features are characteristic of a pentacoordinated species.[16] Additional titrations using MgTPP at higher concentration were performed to monitor the spectral changes in the visible range (see Supporting Information Figure S1). The visible band positions revealed a small red shift upon increased addition of C_{60}Im with isosbestic points located at 550, 597, and 603 nm, respectively. These spectral features suggest formation of a pentacoordinated complex, that is, a 1:1 supramolecular complex, under these solution conditions. Additionally, a Job plot of method of continuous variation also confirmed the 1:1 molecular stoichiometry of the MgP:ImC_{60} supramolecular complex.

Our attempts to obtain a hexacoordinated 1:2 supramolecular complex between MgTPP and C_{60}Im were not fully successful. This is because the higher concentrations of C_{60}Im utilized to form the hexacoordinated complex masked the spectral features associated with MgTPP absorption bands. Hence, accurate spectral characterization was not possible, although at equilibrium conditions the existence of small amounts of hexacoordinated species is conceivable. It may also be mentioned here that extending the spectral region to 1100 nm revealed no new

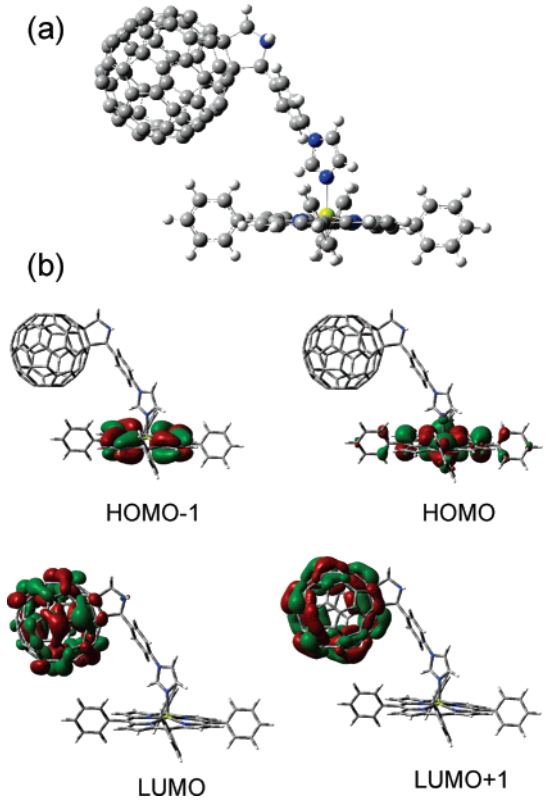

Figure 2. Ab initio B3LYP/3-21G(*) optimized (a) structure (ball-and-stick model) and (b) frontier HOMO−1, HOMO, LUMO, and LUMO+1 orbitals of the C_{60}Im:MgTPP dyad.

charge transfer bands for the C_{60}Im:MgTPP dyad, suggesting the absence of $\pi-\pi$ type interactions between the porphyrin π-system and the fullerene spheroid in the ground states. The Benesi−Hildebrand plot[17] constructed from the absorbance data revealed a straight line with a K_1 value of $(9.2 \pm 0.3) \times 10^3$ M^{-1} (see the Figure 1 inset), indicating fairly stable complex formation. The binding constant, K_1, is larger than the product K_1K_2 for many studied axial ligands.[16] Hence, a large concentration of the complexing agent (1000-fold increase) was needed to observe the hexacoordinated MgTPP complex.

Computational Studies. To gain insight into the molecular geometry and electronic structure, computational studies were performed by using the ab initio B3LYP/3-21G(*) method on the C_{60}Im:MgTPP dyad. We have selected a DFT method over a Hartee Fock method because of the former's accuracy in predicting physicochemical properties as demonstrated on a number of molecular and supramolecular complexes.[9−12] For this, first, both of the starting compounds, MgTPP and C_{60}Im, were fully optimized to a stationary point on the Born−Oppenheimer potential energy surface and allowed to interact. The geometric parameters of the conjugates were obtained after complete energy minimization. Figure 2 shows the calculated B3LYP/3-2G(*) structures for the C_{60}Im:MgTPP dyad. The Mg ← N distance of the newly formed axial coordination bond was computed to be ∼2.06 Å which was similar to the bond distances of the four other Mg−N bonds of the magnesium porphyrin ring. The Mg was pulled out of the porphyrin ring by about 0.45 Å after axial bond formation. From the X-ray structural data, the pulling of the metal out of the porphyrin plane in the case of 1:1 adducts, having square pyramidal geometry, is well-known.[18] The center-to-center distance, that is, the distance between the central magnesium and the center of the C_{60} spheroid, was computed to be ∼12.42 Å, while the edge-to-edge distance between the porphyrin macrocycle and the C_{60} entity was found to be 8.99 Å. These values are not significantly different from those reported earlier for the ZnP:ImC_{60} dyad.[10] The B3LYP/3-21G* calculated gas phase bond dissociation energy for the newly formed axial coordinate bond, that is, the energy difference between the dyad and the sum of the energies of MgTPP and C_{60}Im, was found to be 124.3 kJ mol^{-1}. No basis set superposition error (BSSE) corrections were made, so it is probable that this value is too high (but can be compared to earlier dissociation energies calculated by the same method).[10,11]

The frontier highest occupied frontier molecular orbitals (HOMOs) and lowest unoccupied molecular orbitals (LUMOs) for the investigated dyad were also obtained by the B3LYP/3-21G(*) method, as shown in Figure 2b. The majority of the orbital distributions of the HOMO and HOMO−1 were found to be located on the MgTPP entity with a small orbital coefficient on the axial imidazole ligand. On the other hand, the majority of the orbital distributions of the LUMO and LUMO+1 were located on the C_{60} spheroid. The absence of HOMOs on C_{60} and LUMOs on the porphyrin macrocycle suggests weak or no charge transfer interactions between the MgTPP and C_{60}Im entities in the ground state. These results also suggest that the charge-separated state in electron transfer reactions of the supramolecular complex is $C_{60}Im^{\bullet-}$:$MgTPP^{\bullet+}$. The orbital energies of the HOMO and LUMO were found to be −4.61 and −3.52 eV which resulted in a gas phase "HOMO−LUMO gap" of 1.09 eV. This HOMO−LUMO gap agreed fairly with the electrochemically measured HOMO−LUMO gap (difference between the first oxidation and first reduction potential) (vide infra).

Electrochemical Studies and Electron Transfer Driving Force. Determination of the redox potentials of the newly formed donor−acceptor dyad is important to evaluate the energetics of electron transfer reactions and to probe the existence of charge transfer interactions between the donor and acceptor in the ground state. With this in mind, we have performed a systematic study to evaluate the redox behavior of the self-assembled dyad using the cyclic voltammetric technique. In *o*-dichlorobenzene containing 0.1 M $(n\text{-}C_4H_9)_4NClO_4$, MgTPP revealed two oxidations located at $E_{1/2}$ = 0.07 and 0.46 V versus Fc/Fc^+, respectively. On the basis of the peak-to-peak separation, ΔE_{pp}, values and the cathodic-to-anodic peak current ratio, both of the redox processes of MgTPP were found to be electrochemically and chemically reversible.[19] The first reversible reduction of MgTPP was located at −2.12 V. An irreversible cathodic prewave located at E_{pc} = −2.03 V was also observed. The identity of this prewave was not fully clear. The first oxidation potential of MgTPP located at 0.07 V compares with the first oxidation potential of ZnTPP at 0.28 V under similar solution conditions. The 210 mV easier oxidation of MgTPP implies a better electron donor ability of MgTPP in donor−acceptor systems.

Addition of C_{60}Im revealed an anodic shift of the first oxidation process of MgTPP, as shown in Figure 3. After addition of about 2.2 equiv of C_{60}Im, a new redox process at $E_{1/2}$ = 0.17 V versus Fc/Fc^+ corresponding to the first oxidation of axially ligated MgTPP was observed. No significant change in the second oxidation potential of MgTPP was noticed. The 100 mV anodic shift of the first oxidation potential of MgTPP upon addition of C_{60}Im is noteworthy, since similar titrations involving ZnPTP and C_{60}Im result in changes of less than 20 mV.[10] The reduction potentials of C_{60}Im upon coordination to MgTPP did not reveal any significant changes, suggesting the absence of $\pi-\pi$ type charge transfer interactions between the porphyrin and C_{60} entities. The HOMO−LUMO gap calculated

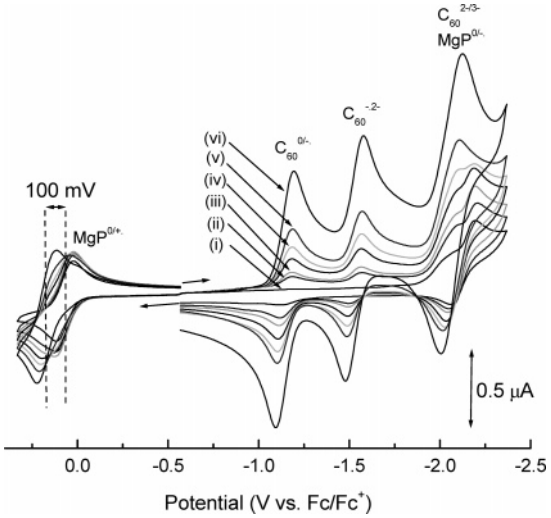

Figure 3. Cyclic voltammograms of MgTPP (0.05 mM) in the presence of (i) 0.25, (ii) 0.50, (iii) 0.75, (iv) 1.0, (v) 1.6, and (vi) 2.2 equiv of C_{60}Im in *o*-dichlorobenzene containing 0.1 M $(n\text{-}C_4H_9)_4NClO_4$. Scan rate 100 mV s^{-1}. The site of electron transfer corresponding to each redox couple is shown on the top of the voltammograms.

using the first oxidation of MgTPP and the first reduction of C_{60} in the dyad was found to be 1.21 V which agrees fairly well with the computationally calculated gas phase HOMO−LUMO gap of 1.09 V.

The free-energy change for electron transfer was calculated using the following expression.[20]

$$\Delta G_{CS}^{\circ} = E_{1/2}(\mathrm{MgTPP}^{\bullet+}/\mathrm{MgTPP}) - E_{1/2}(\mathrm{C_{60}Im}/\mathrm{C_{60}Im}^{\bullet-}) - \Delta E_{0-0} + \Delta G_s \quad (1)$$

where $E_{1/2}(\mathrm{MgTPP}^{\bullet+}/\mathrm{MgTPP})$ is the first one-electron oxidation potential of MgTPP, $E_{1/2}(\mathrm{C_{60}Im}/\mathrm{C_{60}Im}^{\bullet-})$ is the first one-electron reduction potential of C_{60}Im, ΔE_{0-0} is the energy of the 0−0 transition energy gap between the lowest excited state and the ground state of MgTPP (^{1}MgTPP*), and ΔG_s refers to the static Coulomb energy in *o*-dichlorobenzene, calculated by using the "dielectric continuum model"[20] according to the following equation:

$$\Delta G_s = e^2/4\pi\epsilon_0\epsilon_s R_{CC} \quad (2)$$

The center-to-center distance, R_{CC}, was calculated for the optimized structure in Figure 2a to be 12.42 Å. The symbols ϵ_0 and ϵ_s represent vacuum permittivity and dielectric constant of solvent used for photochemical and electrochemical studies, respectively. The ΔG_{CS}° value thus calculated for the C_{60}Im:MgTPP dyad was found to be −0.90 eV, indicating exothermic photoinduced electron transfer from ^{1}MgTPP* to C_{60} in *o*-dichlorobenzene.

Photoinduced Electron Transfer from Singlet Excited Magnesium Porphyrin to Fulleropyrrolidine within the Supramolecular Complex. *Steady State Fluorescence Studies.* The photochemical behavior of the C_{60}Im:MgTPP dyad was investigated, first, by using steady state fluorescence measurements. In argon saturated *o*-dichlorobenzene, MgTPP revealed two emission bands located at 613 and 667 nm, corresponding to the (0,0) and (0,1) transitions, respectively. These emission bands are red shifted by 15−20 nm when compared to the corresponding ZnTPP emission bands under similar solution conditions. Upon addition of C_{60}Im to argon saturated *o*-dichlorobenzene of MgTPP, the fluorescence intensity decreased

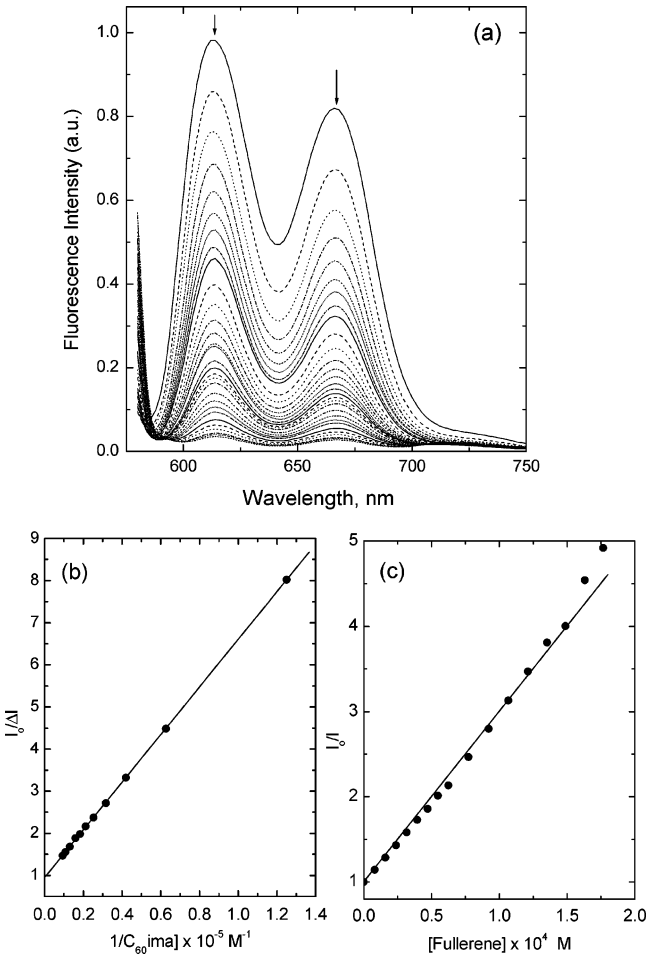

Figure 4. (a) Fluorescence spectra of MgTPP (5.85 μM) in the presence of various amounts of C_{60}Im (8.78 μM each addition) in *o*-dichlorobenzene (λ_{ex} = 565 nm). (b) Benesi−Hildebrand analysis of the fluorescence data. (c) Stern−Volmer plot for the fluorescence quenching of MgTPP at 615 nm by C_{60}Im.

over 95% of the initial intensity (Figure 4). Scanning the emission wavelength to longer wavelength regions (700−775 nm) revealed a weak emission band at 720 nm corresponding to the singlet emission of the fulleropyrrolidine moiety (quantum yield ~10^{-4}). The intensity of this band increased with increased concentration of fulleropyrrolidine. This could either be due to the direct excitation of C_{60}Im at the excitation wavelength of MgTPP or due to the occurrence of energy transfer from ^{1}MgTPP* to C_{60}Im. Changing the excitation wavelength from 567 to 420 nm also revealed similar observations with slightly enhanced emission of fulleropyrrolidine due to its higher absorbance at 420 nm.

The binding constant for the supramolecular complex formation was evaluated by constructing a Benesi−Hildebrand plot[17] of the quenching data. As shown in Figure 4b, such a plot yielded a straight line in the employed concentration range which is in agreement with the formation of the 1:1 supramolecular complex. The binding constant, K_1, calculated was found to be $(1.5 \pm 0.3) \times 10^4$ M^{-1}, which is in agreement with that calculated from the optical data shown in Figure 1.

Figure 4c shows the Stern−Volmer plot for the quenching of MgTPP by C_{60}Im. The plot revealed a higher slope, indicating the occurrence of efficient quenching. The K_{sv} value calculated from the linear segment of the plot was found to be 2.8×10^4 M^{-1}, from which the quenching rate constant, k_q, was calculated to be 5.6×10^{12} M^{-1} s^{-1} by employing a fluorescence lifetime of 5 ns for ^{1}MgTPP*. This k_q value is nearly 3 orders of

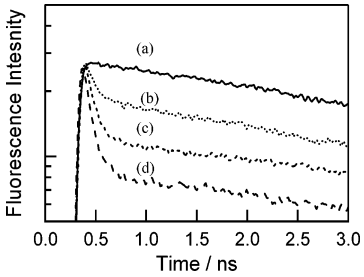

Figure 5. Fluorescence decay profiles of MgTPP (0.03 mM) at 615 nm in the presence of (a) 0.0, (b) 0.10, (c) 0.30, and (d) 0.60 mM C_{60}Im in *o*-dichlorobenzene. $\lambda_{ex} = 400$ nm.

TABLE 1: Fluorescence Lifetimes, τ_f, and Fractions of Fast and Slow Components in *o*-Dichlorobenzene

compound	τ_f[a]/ns (fraction%)	fraction of C_{60}Im:MgTPP from *K* value[b]
MgTPP	5.0 (100%)	0%
C_{60}Im:MgTPP (0.05:0.03 in mM)	0.09 (36%), 5.0 (64%)	28%
C_{60}Im:MgTPP (0.10:0.03 in mM)	0.09 (50%), 5.0 (50%)	56%
C_{60}Im:MgTPP (0.20:0.03 in mM)	0.09 (50%), 5.0 (50%)	63%
C_{60}Im:MgTPP (0.30:0.03 in mM)	0.09 (76%), 5.0 (24%)	72%
C_{60}Im:MgTPP (0.60:0.03 in mM)	0.09 (82%), 5.0 (18%)	84%

[a] See text for details. [b] $K_1 = 9.2 \times 10^3$ M^{-1} from the Figure 1 inset.

magnitude higher than what was expected for intermolecular type diffusion controlled quenching ($k_{diff} = 3.6 \times 10^9$ M^{-1} s^{-1} in *o*-dichlorobenzene ($\eta = 1.32$ cP)). These results clearly demonstrate the occurrence of an intramolecular quenching process in the C_{60}Im:MgTPP supramolecular dyad.

Further, the fluorescence of C_{60}Im was monitored at 720 nm by exciting the samples at 380 nm where the majority of the fulleropyrrolidine was excited. It was observed that in *o*-dichlorobenzene upon addition of an excess of MgTPP (10 equiv), the emission intensity of fulleropyrrolidine at 720 nm was quenched less than 5% of its original intensity. This result suggests the absence of appreciable photochemical events occurring from the singlet excited fulleropyrrolidine to the bound MgTPP, an observation similar to that reported earlier for the C_{60}Im:ZnTPP dyad.[10]

To further evaluate the kinetics of photoinduced processes and to characterize the photochemical products, picosecond time-resolved emission and nanosecond transient absorption studies were performed on the C_{60}Im:MgTPP dyad.

Picosecond Time-Resolved Emission Studies. The fluorescence decay time profile of MgTPP monitored at 613 nm revealed a monoexponential decay (Figure 5), from which the fluorescence lifetime, τ_f, of MgTPP was evaluated to be 5.0 ns. The relatively long-lived singlet excited state of MgTPP compared to the lifetime of the widely used ZnTPP (2.1 ns in *o*-dichlorobenzene) in donor−acceptor dyads shows the importance of MgTPP being a better photosensitizer.

The time-resolved fluorescence spectral features of the C_{60}Im:MgTPP dyad tracked those of the steady state measurements, and the emission decay could be fitted satisfactorily to a biexponential decay. The fast decaying component had a lifetime, τ_f, of 0.09 ns, while the slow decaying component had a lifetime, τ_f, of 5.0 ns which is close to that of pristine MgTPP. Increasing the concentration of C_{60}Im increased the fraction of the fast decaying component (Table 1), thus confirming that this component is due to the presence of C_{60}Im:MgTPP in solution. Indeed, the fractions of the short fluorescence lifetimes are in good agreement with those calculated using K_1, as listed in Table 1.

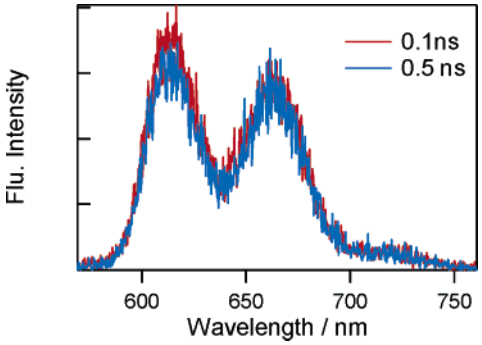

Figure 6. Time-resolved fluorescence spectra of C_{60}Im:MgTPP (0.10:0.03 in mM) in *o*-dichlorobenzene.

The quenching in *o*-dichlorobenzene could occur either from a charge separation process or from an energy transfer process from ^{1}MgTPP* to C_{60}Im within the supramolecular complex. The calculated negative ΔG_{CS} values support the charge separation process in *o*-dichlorobenzene. Additionally, time-resolved emission studies were performed to examine the occurrence of an energy transfer process from ^{1}MgTPP* to C_{60}Im. As shown in Figure 6, the time-resolved emission spectrum recorded at a time interval of 0.5 ns did not reveal appreciable fluorescence enhancement of the fulleropyrrolidine moiety around 720 nm as compared to that obtained at a time interval of 0.1 ns. This result suggests energy transfer from ^{1}MgTPP* to C_{60}Im is not a likely mechanism of fluorescence quenching in the studied supramolecular dyad.

By assuming that the quenching is due to electron transfer from the singlet excited MgTPP to C_{60}Im, which has been proved by the transient absorption methods in the next section, the rate of charge separation, $k_{CS}^{singlet}$, and quantum yields, $\Phi_{CS}^{singlet}$, were evaluated according to eqs 3 and 4 for the intramolecular electron transfer process.

$$k_{CS}^{singlet} = (1/\tau_f)_{sample} - (1/\tau_f)_{ref} \quad (3)$$

$$\Phi_{CS}^{singlet} = [(1/\tau_f)_{sample} - (1/\tau_f)_{ref}]/(1/\tau_f)_{sample} \quad (4)$$

The measured $k_{CS}^{singlet}$ and $\Phi_{CS}^{singlet}$ values were found to be 1.1×10^{10} s^{-1} and 0.99 in *o*-dichlorobenzene. This $k_{CS}^{singlet}$ value compared with a value of 1.7×10^{10} s^{-1} for the C_{60}Im:ZnTPP dyad[10] and 8.9×10^9 s^{-1} for the C_{60}Im:ZnNc dyad (where ZnNc = zinc 2,11,20,29-tetra-*tert*-butyl-2,3-naphthalocyanine).[11] The slightly higher $k_{CS}^{singlet}$ value in the case of C_{60}Im:MgTPP indicates efficient charge separation in the studied dyad. It may be mentioned here that changing the solvent to toluene had virtually no effect on the kinetic data of the supramolecular dyad.

Nanosecond Transient Absorption Spectral Studies. Evidence for charge separation and the rate of charge recombination, k_{CR}, were obtained from nanosecond transient absorption spectral studies using a 532 nm laser light. Figure 7 shows the transient absorption spectrum of a mixture of MgTPP and C_{60}Im in *o*-dichlorobenzene at 10 and 100 ns time intervals. Absorption bands corresponding to the triplet states of MgTPP (^{3}MgTPP*) and C_{60} ($^3C_{60}$*) entities were observed at 840 and 700 nm, respectively.[21−23] Importantly, peaks corresponding to the formation of the magnesium porphyrin cation radical ($MgTPP^{\bullet+}$) around the 650−700 nm region[22] and the fulleropyrrolidine anion radical ($C_{60}Im^{\bullet-}$) around 1020 nm,[8,10] as evidence for the occurrence of photoinduced electron transfer in this dyad, were observed. As shown in the Figure 7 inset, the time profile of the 1020 nm peak showed a quick rise−decay, indicating

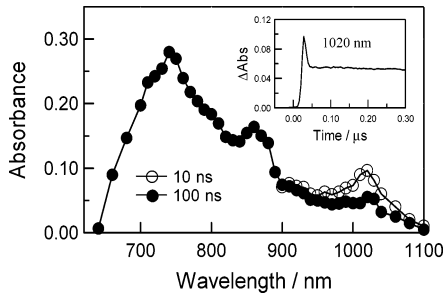

Figure 7. Transient absorption spectra of a mixture of MgTPP (0.10 mM) and C_{60}Im (0.40 mM) in Ar-saturatred *o*-dichlorobenzene obtained by 532 nm laser light excitation.

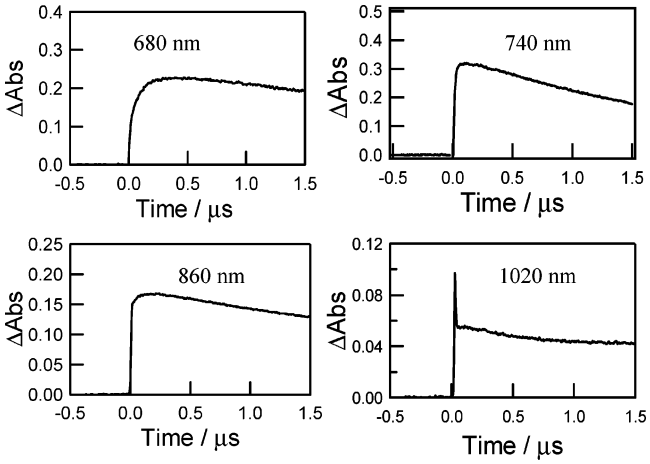

Figure 8. Time profiles of transient absorption bands of C_{60}Im:MgTPP (0.20:0.10 in mM) in Ar-saturatred *o*-dichlorobenzene after 532 nm laser light excitation.

supramolecular ion-pair formation via the singlet state of MgTPP. In *o*-dichlorobenzene, the decay of $C_{60}^{\bullet-}$ around 1020 nm was in the nanosecond range which is shorter than the decay of the ^{3}MgTPP* and $^3C_{60}$* entities. From the decay of the 1020 nm band (Figure 7 inset), the k_{CR} value of $C_{60}Im^{\bullet-}$:$MgTPP^{\bullet+}$ was evaluated to be $(8.5 \pm 0.3) \times 10^7$ s^{-1} in *o*-dichlorobenzene.

The time profiles of the transient absorption bands at different wavelengths of the C_{60}Im:MgTPP dyad after 532 nm laser light excitation are shown in Figure 8. In the time profiles at longer time scale, the decay rates of the triplet states of the MgTPP and C_{60} entities monitored at 860 and 740 nm, respectively, showed slow decay corresponding to lifetimes in the range 20−50 μs. The absorption peak of $MgTPP^{\bullet+}$ monitored at 680 nm showed a slow rise instead of the quick rise of $C_{60}Im^{\bullet-}$ at 1020 nm, probably due to the effect of emission of MgTPP in the 600−700 nm region. The slow decay at 1020 nm after 50 ns may be attributed to the absorption tail of ^{3}MgTTP*.

Earlier, a k_{CR} value of $<10^8$ s^{-1} was obtained for $C_{60}Im^{\bullet-}$:$ZnTPP^{\bullet+}$ in *o*-dichlorobenzene,[10] while such values for a structurally similar supramolecular system, $C_{60}Im^{\bullet-}$:$ZnNc^{\bullet+}$, were 9.2×10^7 and 5.3×10^7 s^{-1}, respectively, in *o*-dichlorobenzene and toluene.[11] Using k_{CS} and k_{CR} calculated for the C_{60}Im:MgTPP dyad, the ratio k_{CS}/k_{CR} was evaluated as a measure of the excellence of photoinduced electron transfer and was found to be in the range 125−130. These values are slightly better than the values obtained for C_{60}Im:ZnNc ($k_{CS}/k_{CR} = \sim 100$)[11] and are better by an order of magnitude than the value reported for the C_{60}Im:ZnTPP dyad.[10] These results suggest a better opportunity to utilize the $C_{60}Im^{\bullet-}$:$MgTPP^{\bullet+}$ charge-separated state for further electron-mediating processes. However, in general, the k_{CR} values for the supramolecular systems held by metal−ligand coordination are larger than those

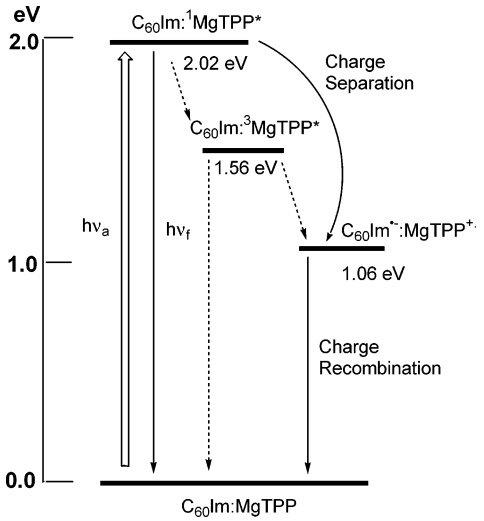

Figure 9. Energy level diagram showing photochemical events of the supramolecular C_{60}Im:MgTPP dyad in *o*-dichlorobenzene.

held by covalent bonds.[8] This is probably due to a relatively large electronic coupling matrix element between the central metal atom of the porphyrin cavity and imidazole pendant of the fulleropyrrolidine.

Energy Level Diagram and Summary. The spectral studies performed revealed fairly stable, 1:1 supramolecular C_{60}Im:MgTPP dyad formation in *o*-dichlorobenzene. Although a 1:2 supramolecular complex was not fully possible to form and characterize, the present spectral, electrochemical, and photochemical studies have provided interesting results in contrast to the earlier studied C_{60}Im:ZnTPP and C_{60}Im:ZnNc supramolecular dyads. Fine-tuning of the HOMO energy level (first oxidation) upon pentacoordinated complex formation has been demonstrated for the studied dyad using cyclic voltammetric studies.

The energy level diagram constructed by utilizing the spectral, electrochemical, and photochemical data of the studied supramolecular dyad in *o*-dichlorobenzene is illustrated in Figure 9. The free-energy calculations, steady-state and time-resolved emission, and transient absorption studies have revealed the occurrence of electron transfer from the singlet excited MgTPP to the coordinated C_{60}Im, resulting in the formation of $C_{60}Im^{\bullet-}$:$MgTPP^{\bullet+}$. The measured rate constant ($k_{ET} = 1.1 \times 10^{10}$ s^{-1}) and the quantum yield ($\Phi_{CS} = 0.99$) indicate efficient formation of $C_{60}Im^{\bullet-}$:$MgTPP^{\bullet+}$ upon excitation of the magnesium porphyrin in the self-assembled dyad. The nanosecond transient absorption spectrum of the C_{60}Im:MgTPP dyad exhibited the characteristic peak of $C_{60}^{\bullet-}$ at 1020 nm. The measured k_{CR} value indicated a higher opportunity to utilize the charge-separated state for further electron-mediating processes, a property that is better than that earlier reported for C_{60}Im:ZnTPP and C_{60}Im:ZnNc dyads.

The relative energy levels of the charge-separated states of $C_{60}Im^{\bullet-}$:$MgTPP^{\bullet+}$ and the earlier reported $C_{60}Im^{\bullet-}$:$ZnTPP^{\bullet+}$ [10] and $C_{60}Im^{\bullet-}$:$ZnNc^{\bullet+}$ [11] are suggestive of the magnitude of energy storage in these dyads. These values are found to be 1.06 eV for C_{60}Im:MgTPP, 1.26 eV for C_{60}Im:ZnTPP, and 0.89 eV for C_{60}Im:Nc. The energy level diagram also suggests the possibility of electron transfer from ^{3}MgTPP* formed after undergoing intersystem crossing of ^{1}MgTPP*. In the present study, we have not observed such electron transfer from the triplet excited metalloporphyrin probably due to the very efficient charge separation ($\Phi_{CS}^{singlet} \sim 1.0$) from the singlet excited states of the dyad.

Experimental Section

Chemicals. Buckminsterfullerene (C_{60}, +99.95%) was from SES Research, (Houston, TX). *o*-Dichlorobenzene and toluene in sure seal bottles were from Aldrich Chemicals (Milwaukee, WI). Tetra-*n*-butylammonium perchlorate ($(n\text{-}C_4H_9)_4NClO_4$) was from Fluka Chemicals. The syntheses and purification of MgTPP[24] and C_{60}Im[10] were carried out according to literature procedures.

Instrumentation. The UV−visible spectral measurements were carried out with a Shimadzu model 1600 UV−visible spectrophotometer. The fluorescence emission was monitored by using a Spex Fluorolog-tau spectrometer. A right angle detection method was used. Cyclic voltammograms were recorded on a EG&G model 263A potentiostat using a three-electrode system. A platinum button or glassy carbon electrode was used as the working electrode. A platinum wire served as the counter electrode and Ag/AgCl was used as the reference electrode. A ferrocene/ferrocenium redox couple was used as an internal standard. All the solutions were purged prior to electrochemical and spectral measurements using argon gas. The computational calculations were performed by ab initio B3LYP/3-21G(*) methods with the Gaussian 03 software package on high speed computers.[25] The images of the frontier orbitals were generated from Gauss View 03 software.

Time-Resolved Emission and Transient Absorption Measurements.[26] The picosecond time-resolved fluorescence spectra were measured using an argon-ion pumped Ti:sapphire laser (Tsunami) and a streak scope (Hamamatsu Photonics). Nanosecond transient absorption spectra in the near-IR region were measured by means of laser-flash photolysis; 532 nm light from a Nd:YAG laser was used as an exciting source and a Ge-avalanche-photodiode module was used for detecting the monitoring light from a pulsed Xe lamp as described in our previous reports.[26]

Acknowledgment. The authors are thankful to the donors of the Petroleum Research Fund administered by the American Chemical Society and National Institutes of Health (GM 59038), Grants-in-Aid for Scientific Research on Priority Area (417) from the Ministry of Education, Science, Sport and Culture of Japan (to O.I. and Y.A.), and a Grant-in-Aid for the COE project Giant Molecules and Complex Systems (to M.E.E.) for support of this work.

Supporting Information Available: Visible spectral changes observed for C_{60}Im binding to MgTPP in *o*-dichlorobenzene. This material is available free of charge via the Internet at http://pubs.acs.org.

References and Notes

(1) (a) *The Photosynthetic Reaction Center*; Deisenhofer, J., Norris, J. R., Eds.; Academic Press: San Diego, CA, 1993. (b) Deisenhofer, J.; Epp, O.; Miki, K.; Huber, R.; Michel, H. *J. Mol. Biol.* **1984**, *180*, 385. (c) Kirmaier, C.; Holton, D. In *The Photosynthetic Reaction Center*; Deisenhofer, J., Norris, J. R., Eds.; Academic Press: San Diego, CA, 1993; Vol. II, pp 49−70.

(2) (a) McLendon, G.; Hake, R. *Chem. Rev.* **1992**, *92*, 481. (b) Lewis, F. D.; Letsinger, R. L.; Wasielewski, M. R. *Acc. Chem. Res.* **2001**, *34*, 159.

(3) (a) Miller, J. R.; Calcaterra, L. T.; Closs, G. L. *J. Am. Chem. Soc.* **1984**, *106*, 3047. (b) Closs, G. L.; Miller, J. R. *Science* **1988**, *240*, 440. (c) Connolly, J. S.; Bolton, J. R. In *Photoinduced Electron Transfer*; Fox, M. A., Chanon, M., Eds.; Elsevier: Amsterdam, The Netherlands, 1988; Part D, pp 303−393. (d) Wasielewski, M. R. In *Photoinduced Electron Transfer*; Fox, M. A., Chanon, M., Eds.; Elsevier: Amsterdam, The Netherlands, 1988; Part A, pp 161−206.

(4) (a) Wasielewski, M. R. *Chem. Rev.* **1992**, *92*, 435. (b) Gust, D.; Moore, T. A.; Moore, A. L. *Acc. Chem. Res.* **1993**, *26*, 198. (c) Kurreck, H.; Huber, M. *Angew. Chem., Int. Ed. Engl.* **1995**, *34*, 849. (d) Gust, D.; Moore, T. A.; Moore, A. L. *Acc. Chem. Res.* **2001**, *34*, 40.

(5) (a) Harriman, A.; Sauvage, J.-P. *Chem. Soc. Rev.* **1996**, *26*, 41. (b) Blanco, M.-J.; Jiménez, M. C.; Chambron, J.-C.; Heitz, V.; Linke, M.; Sauvage, J.-P. *Chem. Soc. Rev.* **1999**, *28*, 293. (c) Balzani, V.; Juris, A.; Venturi, M.; Campagna, S.; Serroni, S. *Chem. Rev.* **1996**, *96*, 759. (d) *Electron Transfer in Chemistry*; Balzani, V., Ed.; Wiley-VCH: Weinheim, Germany, 2001.

(6) (a) Paddon-Row: M. N. *Acc. Chem. Res.* **1994**, *27*, 18. (b) Verhoeven, J. W. *Adv. Chem. Phys.* **1999**, *106*, 603. (c) Maruyama, K.; Osuka, A.; Mataga, N. *Pure Appl. Chem.* **1994**, *66*, 867. (d) Osuka, A.; Mataga, N.; Okada, T. *Pure Appl. Chem.* **1997**, *69*, 797. (e) Sun, L.; Hammarström, L.; Åkermark, B.; Styring, S. *Chem. Soc. Rev.* **2001**, *30*, 36.

(7) (a) Sessler, J. S.; Wang, B.; Springs, S. L.; Brown, C. T. In *Comprehensive Supramolecular Chemistry*; Atwood, J. L., Davies, J. E. D., MacNicol, D. D., Vögtle, F., Eds.; Pergamon: 1996; Chapter 9. (b) Hayashi, T.; Ogoshi, H. *Chem. Soc. Rev.* **1997**, *26*, 355. (c) Ward, M. W. *Chem. Soc. Rev.* **1997**, *26*, 365. (d) Piotrowiak, P. *Chem. Soc. Rev.* **1999**, *28*, 143.

(8) (a) Imahori, H.; Sakata, Y. *Adv. Mater.* **1997**, *9*, 537. (b) Prato, M. *J. Mater. Chem.* **1997**, *7*, 1097. (c) Martín, N.; Sánchez, L.; Illescas, B.; Pérez, I. *Chem. Rev.* **1998**, *98*, 2527 (d) Diederich, F.; Gómez-López, M. *Chem. Soc. Rev.* **1999**, *28*, 263. (e) Imahori, H.; Sakata, Y. *Eur. J. Org. Chem.* **1999**, 2445. (f) Guldi, D. M. *Chem. Commun.* **2000**, 321. (g) Guldi, D. M.; Prato, M. *Acc. Chem. Res.* **2000**, *33*, 695. (h) Guldi, D. M.; Kamat, P. V. In *Fullerenes*; Kadish, K. M., Ruoff, R. S., Eds.; John Wiley & Sons: New York, 2000; Chapter 5, pp 225−281. (i) Guldi, D. M. *Chem. Soc. Rev.* **2002**, *31*, 22. (j) Meijer, M. D.; van Klink, G. P. M.; van Koten, G. *Coord. Chem. Rev.* **2002**, *230*, 141. (k) El-Khouly, M. E.; Ito, O.; Smith, P. M.; D'Souza, F. *J. Photochem. Photobiol., C* **2004**, *5*, 79. (l) Imahori, H.; Fukuzmi, S. *Adv. Funct. Mater.* **2004**, *14*, 525. (m) Boyd, P. D.; Reed, C. A. *Acc. Chem Res.*, published online Dec 7, http://dx.doi.org/10.1021/ar040168f.

(9) D'Souza, F.; Ito, O. *Coord. Chem. Rev.*, in press.

(10) D'Souza, F.; Deviprasad, G. R.; Zandler, M. E.; Hoang, V. T.; Arkady, K.; Van Stipdonk, M.; Perera, A.; El-Khouly, M. E.; Fujitsuka, M.; Ito, O. *J. Phys. Chem. A* **2002**, *106*, 3243.

(11) El-Khouly, M. E.; Rogers, L. M.; Zandler, M. E.; Suresh, G.; Fujitsuka, M.; Ito, O.; D'Souza, F. *ChemPhysChem* **2003**, *4*, 474.

(12) (a) D'Souza, F.; Deviprasad, G. R.; Rahman, M. S.; Choi, J.-P. *Inorg. Chem.* **1999**, *38*, 2157. (b) D'Souza, F.; Rath, N. P.; Deviprasad, G. R.; Zandler, M. E. *Chem. Commun*. **2001**, 267. (c) D'Souza, F.; Deviprasad, G. R.; El-Khouly, M. E.; Fujitsuka, M.; Ito, O. *J. Am. Chem. Soc.* **2001**, *123*, 5277. (d) D'Souza, F.; Deviprasad, G. R.; Zandler, M. E.; El-Khouly, M. E.; Fujitsuka, M.; Ito, O. *J. Phys. Chem. B* **2002**, *106*, 4952. (e) D'Souza, F.; Deviprasad, G. R.; Zandler, M. E.; El-Khouly, M. E.; Fujitsuka, M.; Ito, O. *J. Phys. Chem. A* **2003**, *107*, 4801. (f) El-Khouly, M. E.; Gadde, S.; Deviprasad, G. R.; Fujitsuka, M.; Ito, O.; D'Souza, F. *J. Porphyrins Phthalocyanines* **2003**, *7*, 1. (g) D'Souza, F.; Smith, P. M.; Zandler, M. E.; McCarty, A. L.; Itou, M.; Araki, Y.; Ito, O. *J. Am. Chem. Soc.* **2004**, *126*, 7898. (h) D'Souza, F.; Smith, P. M.; Gadde, S.; McCarty, A. L.; Kullman, M. J.; Zandler, M. E.; Itou, Y.; Araki, Y.; Ito, O. *J. Phys. Chem. B* **2004**, *108*, 11333. (i) D'Souza, F.; Gadde, S.; Zandler, M. E.; Itou, M.; Araki, Y.; Ito, O. *Chem. Commun*. **2004**, 2276. (j) D'Souza, F.; Chitta, R.; Gadde, S.; Zandler, M. E.; Sandanayaka, A. S. D.; Araki, Y.; Ito, O. *Chem. Commun*. **2005**, 1279.

(13) (a) Armaroli, N.; Diederich, F.; Echegoyen, L.; Habicher, T.; Flamigni, L.; Marconi, G.; Nierengarten,. J.-F. *New. J. Chem.* **1999**, 77. (b) Da Ros, T.; Prato, M.; Guldi, D. M.; Alessio, E.; Ruzzi, M.; Pasimeni, L. *Chem. Commun*. **1999**, 635. (c) Da Ros, T.; Prato, M.; Guldi, D. M.; Ruzzi, M.; Pasimeni, L. *Chem.−Eur. J.* **2001**, *7*, 816. (d) Hauke, F.; Swartz, A.; Guldi, D. M.; Hirsh, A. *J. Mater. Chem*. **2002**, *12*, 2088. (e) Wilson, S. R.; MacMahon, S.; Tat, F. T.; Jarowski, P. D.; Schuster, D. I. *Chem. Commun*. **2003**, 226. (f) Kim, H. J.; Park, K.-M.; Ahn, K.; Kum S. K.; Kim, S.; Kim, D.; Kim, H.-J. *Chem. Commun*. **2004**, 2594. (g) Sessler, J. L.; Jayawickramarajah, J.; Gouloumis, A.; Torres, T.; Guldi, D. M.; Maldonado, S.; Stevenson, K. J. *Chem. Commun.* **2005**, advanced article.

(14) *The Porphyrin Handbook*; Kadish, K. M., Smith, K. M., Guilard, R., Eds.; Academic Press: Burlington, MA, 2000; Vols. 1−10.

(15) (a) Dorough, G. D.; Miller, J. R.; Huennekens, F. M. *J. Am. Chem. Soc*. **1951**, *73*, 4315. (b) Allison, J. B.; Becker, R. S. *J. Chem. Phys*. **1960**, *32*, 1410.

(16) (a) Miller, J. R.; Dorough, G. D. *J. Am. Chem. Soc*. **1952**, *74*, 3977. (b) Kadish, K. M.; Shiue, L. R. *Inorg. Chem*. **1982**, *21*, 1112.

(17) Benesi, H. A.; Hildebrand, J. H. *J. Am. Chem. Soc*. **1949**, *71*, 2703.

(18) Hoard, J. L. *Science (Washington, D.C.)* **1971**, *174*, 1295.

(19) Bard, A. J., Faulkner, L. R. *Electrochemical Methods: Fundamentals and Applications*, 2nd ed.; John Wiley: New York, 2001.

(20) (a) Rehm, D.; Weller, A. *Isr. J. Chem.* **1970**, *7*, 259. (b) Mataga, N.; Miyasaka, H. In *Electron Transfer*; Jortner, J., Bixon, M., Eds.; John Wiley & Sons: New York, 1999; Part 2, pp 431−496.

(21) (a) Harriman, A.; Neta, P.; Richoux, M.-C. *J. Phys. Chem*. **1986**, *90*, 3444. (b) Skillman, A. G.; Collins, J. R.; Loew, G. H. *J. Am Chem. Soc*. **1992**, *114*, 9538.

(22) Nojiri, T.; Watanabe, A.; Ito, O. *J. Phys. Chem. A* **1998**, *102*, 5215.

(23) (a) Ghosh, H. N.; Pal, H.; Sapre, A. V.; Mittal J. P. *J. Am. Chem. Soc*. **1993**, *115*, 11722. (b) Fujitsuka, M.; Ito, O.; Yamashiro, T.; Aso, Y.; Otsubo, T. *J. Phys. Chem. A* **2000**, *104*, 4876.

(24) Lindsey, J. S.; Woodford, J. N. *Inorg. Chem*. **1995**, *34*, 1063.

(25) *Gaussian 03*, revision B-04; Gaussian, Inc.: Pittsburgh, PA, 2003.

(26) (a) Matsumoto, K.; Fujitsuka, M.; Sato, T.; Onodera, S.; Ito, O. *J. Phys. Chem. B* **2000**, *104*, 11632. (b) Komamine, S.; Fujitsuka, M.; Ito, O.; Morikawa, K.; Miyata, T.; Ohno, T. *J. Phys. Chem. A* **2000**, *104*, 11497. (c) Yamazaki, M.; Araki, Y.; Fujitsuka, M.; Ito, O. *J. Phys. Chem. A* **2001**, *105*, 8615.